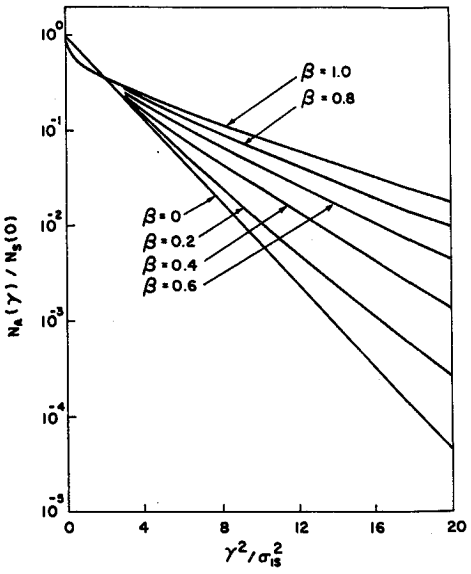

Fig. 4 Normalized time-average expected frequency of the displacement response to variable intensity excitation exceeding various levels, $\zeta = 0.5$.

$$N_A(\gamma) = \int_{t_0}^{\infty} N(\gamma, t)\, dt/(t_f - t_0) \tag{8}$$

For $\gamma^2/\sigma_{1S}{}^2 > 1.5$ this ratio increases with system damping. The curve for $\zeta = 0.5$ practically coincides with stationary values, i.e., $N_S(\gamma)/N_S(0)$, over most of its length. These results indicate that for a lightly damped system, unless the excitation time interval is large, it is necessary to include transient effects to make reliable estimates of exceedance statistics. For the example studied stationary estimates for the expected number of displacement exceedances above high levels are conservative, since the influence of transient motions was to reduce the values of this parameter.

The temporal behavior of the normalized expected frequency of displacement exceedances of the level $\gamma = 3\sigma_{1S}$ for a variable intensity input is illustrated in Fig. 3. The dashed line denotes the stationary value of this parameter. It is readily observed that the number of displacement exceedances above the level $3\sigma_{1S}$ will be greater in the case of the prescribed variable intensity excitation. Curves of the ratio $N_A(\gamma)/N_S(0)$ vs $\gamma^2/\sigma_{1S}{}^2$ for $\zeta = 0.5$ and selected values of β appear in Fig. 4. In this case $N_A(\gamma)$ was obtained by averaging $N(\gamma, t)$ over one period of the modulating function. The average expected frequency of exceeding high levels, $\gamma > 2\sigma_{1S}$, increases as the amplitude of the modulating function increases. This effect is more pronounced at the higher levels and for heavily damped systems. The trends indicated in Fig. 4 are the same as those observed for atmospheric turbulence data,[1,5] i.e., observed values of exceedance frequencies are similar to the $\beta = 0.2$ and $\beta = 0.4$ curves while the theoretical prediction is given by the $\beta = 0$ curve.

References

[1] Dutton, J. A., "Effects of Turbulence on Aeronautical Systems," *Progress in Sciences*, 1st ed., Vol. 11, Pergamon Press, Oxford, England, 1970, pp. 67–109.

[2] Piersol, A. G., "Investigation of the Statistical Properties of Atmospheric Turbulence Data," TR MAC 28032-07, 1969, Measurement Analysis Corp., Marina Del Rey, Calif.

[3] Howell, L. J., "Response of Flight Vehicles to Nonstationary Random Atmospheric Turbulence," Ph.D. thesis, 1971, University of Illinois, Urbana, Ill.

[4] Zadeh, L. A. and Desoer, C. A., *Linear System Theory*, 1st ed., McGraw-Hill, New York, 1963, pp. 294–300.

[5] Atnip, F. K. and Gault, J., "An Analysis of Gust Velocities for Application to Aircraft Design," *International Conference on Atmospheric Turbulence*, Royal Aeronautical Society, London, May, 1971.

Artificial Viscosity Methods for Blunt Body Flowfield Analysis with Thermal Radiation

JAMES O. NICHOLS*
Auburn University, Auburn, Ala.

Nomenclature

e = energy per unit volume
h = computational mesh length
p = pressure
t = time
T = temperature
u_i = velocity in x_i direction
x, y = Cartesian coordinates in direction parallel to and normal to, respectively, the freestream direction
σ = Stefan-Boltzmann constant
σ_0 = constant time-step parameter at initial conditions
ω = constant artificial viscosity parameter

Introduction

ARTIFICIAL viscosity methods have been used to successfully predict flowfields about bodies[1,2] including the effects of angle of attack and nonequilibrium flow. The purpose of this investigation was to determine the effects of including thermal radiation in two of these methods. The two artificial viscosity methods chosen, Lax's[3] and Rusanov's[4] methods, were selected because of their simplicity and because Lax's method assumes a constant artificial viscosity coefficient while Rusanov's method allows the artificial viscosity coefficient to vary with position in the flowfield. A modification to Lax's method is also presented which greatly strengthens the stability of the equations.

The investigation was conducted at two Mach numbers, 10 and 30. The lower was chosen because it represents an approximate lower bound at which thermal radiation may be important and the upper represents the approximate bound for the gray, optically thin gas assumption.

The body chosen for this investigation was a two-dimensional, semi-infinite, planar body with a thickness of 1 ft and a flat leading edge. There are several reasons for choosing this shape. For example, it is a shape not easily adaptable to other methods of solution. Also, heat-transfer analyses have generally considered bodies with convex leading edges; therefore, most heat-transfer data are expressed in terms of nose radius which leaves one at a loss in predicting heat transfer rates to a flat-faced body.

The body was assumed to be at zero angle of attack and the gas was assumed to be not only gray and optically thin, but also thermally and calorically perfect. The only purpose of these assumptions was to reduce the computations.

Modified Lax Method

In the numerical calculations flow properties at a point in the computation net were found by averaging the properties of the four net points surrounding the point. Lax's method uses the properties of the surrounding points at the same time step. This method was modified by using the properties of the points at the current time step calculation; i.e., since the calculations were performed by a forward step in the positive x and y directions, the properties at the net point before and the point below were the properties at time $t+\Delta t$ while the properties of the point after and the point above were the properties at time t. This modification was found to strengthen the stability of the difference equations and also saved computer storage space.

Radiation

To include the effects of heat transfer by radiation in the

Received September 2, 1971; revision received December 23, 1971.
Index category: Radiatively Coupled Flows and Heat Transfer.
* Associate Professor of Aerospace Engineering. Member AIAA.

Table 1 Convergence test ($N = 500$)

Method	Time-step parameter, σ_0	Time step Δt, sec	Computation time, sec
	a) $M = 10$		
Rusanov ($\omega = 1.0$)	0.75	3.1084×10^{-6}	474
Modified lax	0.89	3.6687×10^{-6}	259
Lax	0.88	3.6472×10^{-6}	265
	b) $M = 30$		
Rusanov ($\omega = 1.0$)	0.008	1.1765×10^{-8}	Did not converge
Rusanov ($\omega = 1.5$)	0.46	6.7650×10^{-7}	447
Modified lax	0.64	9.4121×10^{-7}	227
Lax	0.03	4.4119×10^{-8}	Did not converge

analysis of the flowfield, it is necessary to add a heat flux term to the energy equation. This is done by introducing the radiant heat flux vector q_i. The energy equation in Cartesian tensor notation is

$$\partial e/\partial t + \partial[(e+p)u_i]/\partial x_i = -\partial(q_i)/\partial x_i \quad (1)$$

The divergence of the heat flux vector can be written very simply for an optically thin, gray gas.[5] Thus

$$\partial q_i/\partial x_i = 4\alpha\sigma T^4 \quad (2)$$

The value of the gray absorption coefficient α used in these calculations was obtained from Howe.[6] This value of α applies to the test conditions at $M = 10$, but the temperature range for which it is valid does not extend to the temperatures attained in the stagnation region at $M = 30$. Since a perfect gas was assumed, the temperatures computed at $M = 30$ are much higher than would be expected for a real gas. The real gas temperature is only about 20% of the perfect gas temperature in the stagnation region at this Mach number. An approximation was therefore made by multiplying the α obtained from Howe by 10^{-5} in the computations at $M = 30$.

Results and Conclusions

The flowfields without radiation computed by the two artificial viscosity methods and the modified Lax method are first compared on the basis of convergence, computational time, and flowfield agreement. For the convergence test, the computations were required to converge for 500 time steps ($N = 500$). Table 1 shows the results of this test. At $M = 10$, the Lax and modified Lax methods converged for larger time steps than the Rusanov method.

Computations by Lax's method can be made to converge by decreasing the size of the time step, but in Rusanov's method, there are two constants to manipulate. The time step is controlled by the time-step parameter σ_0 and the viscosity by the parameter ω. Computations by Rusanov's method can be made to converge by reducing σ_0 and/or increasing ω. The choices of σ_0 and ω are guided by the stability requirement

$$\sigma_0 \leqq \omega \leqq 1/\sigma_0 \quad (3)$$

At $M = 30$, neither the Lax nor the Rusanov method converged even when the time step was considerably reduced. By increasing ω Rusanov's method was made to converge. The modified Lax method shows a much stronger stability and converged for a time step only about one-third less than required at $M = 10$.

Comparisons of the flowfield properties (velocity, pressure and density) along the stagnation streamline at $M = 10$ show that results from all three methods agree very well, although the properties predicted by the Rusanov method are slightly lower in the shock layer. Flowfield properties computed by the modified Lax method and the Rusanov method at $M = 30$ were in agreement as were the results at $M = 10$ except that the shock wave

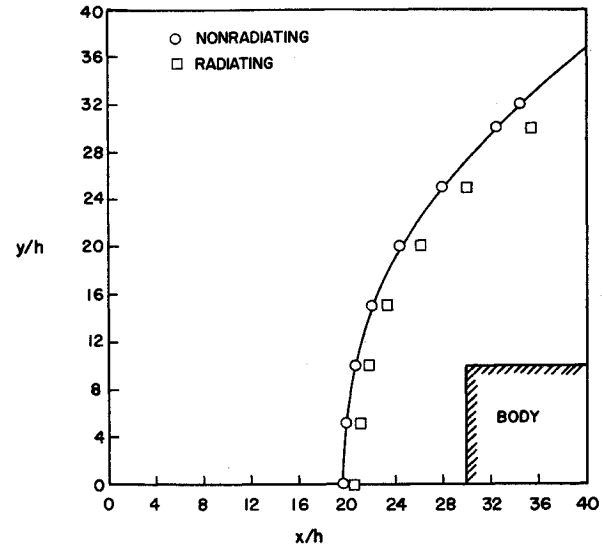

Fig. 1 Shock wave shape and location by modified lax method—radiating and nonradiating flow, $M = 30$.

was smeared out more for Rusanov's method because ω was increased to 1.5.

The viscous effects were confined to the shock wave which was about four or five mesh lengths in thickness at $M = 10$. The shock wave position was found by using the midpoint of the density rise through the shock wave. Figure 1 shows the predicted shock wave shape and position at $M = 30$.

The effects of radiation were found to be similar to those found by other investigators; that is, the shock wave was moved closer to the body as shown in Fig. 1, the pressure and velocity distributions were essentially unaffected, while the temperature in the shock layer was reduced and density was increased (see Fig. 2). The Lax methods agree throughout the

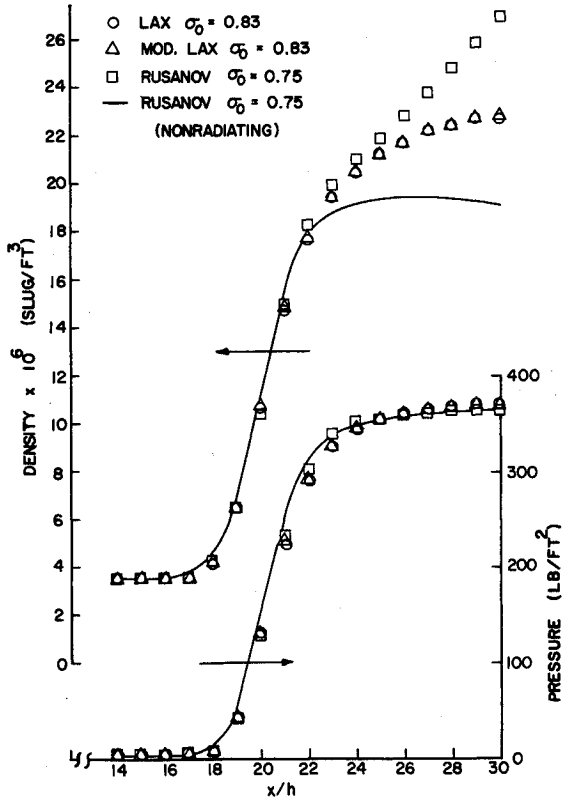

Fig. 2 Stagnation streamline densities and pressures—radiating flow, $M = 10$, $N = 500$.

flowfield while Rusanov's method shows considerable difference in density and temperature in the shock layer. This may be a result of allowing the viscosity to vary.

The addition of heat-transfer terms to the flow equations had little effect on their convergence at $M = 10$; however, at $M = 30$, only the modified Lax method converged even after α was corrected as described in the section on radiation.

References

[1] Bohachevsky, I. O. and Rubin, E. L., "A Direct Method for Computation of Nonequilibrium Flows with Detached Shock Waves," *AIAA Journal*, Vol. 4, No. 4, April 1966, pp. 600–606.

[2] Bohachevsky, I. O. and Mates, R. E., "A Direct Method for Calculation of the Flow about an Axisymmetric Blunt Body at Angle of Attack," *AIAA Journal*, Vol. 4, No. 5, May 1966, pp. 776–782.

[3] Lax, P. D., "Weak Solutions of Nonlinear Hyperbolic Equations and Their Numerical Computation," *Communications on Pure and Applied Mathematics*, Vol. 7, 1954, pp. 159–193.

[4] Holt, M., ed., *Basic Developments in Fluid Dynamics*, Vol. I, Academic Press, New York, 1965, pp. 22–27.

[5] Vincenti, W. G. and Kruger, C. H., Jr., *Introduction to Physical Gas Dynamics*, Wiley, New York, 1965, pp. 436–471.

[6] Howe, J. T., "Radiation Emission Effects of the Equilibrium Boundary Layer in the Stagnation Region," TN D-1030, Sept. 1961, NASA.

Influence of Splitter Plate on Galloping Response of an Angle Section

J. E. SLATER*

Defence Research Establishment Atlantic, Defence Research Board, Dartmouth, Nova Scotia, Canada

AND

V. J. MODI†

University of British Columbia, Vancouver, Canada

Nomenclature

a_1 = coefficient of polynomial curve fit, coefficient 'A' in Ref. 4
h = maximum width of the angle model
k_y = plunging stiffness of the system
ℓ = length of the model
m = mass of the oscillating system
η_y = dimensionless mass parameter, ρh^2 $(2m)$
r_y = viscous damping coefficient in plunging
t = real time
x, y = downstream and transverse co-ordinates, respectively
$\bar{y}$ = amplitude of lateral displacement
U_{0y} = dimensionless critical velocity, $2\beta_y/\eta_y a_1$
$\bar{Y}$ = dimensionless amplitude of the plunging motion
$\bar{Y}^* = \bar{Y}/U_{0y}$
$\bar{Y}_0$ = dimensionless initial amplitude of lateral motion
$\bar{Y}_0^* = \bar{Y}_0/U_0{}^y$
α_0 = mean angle of attack of oscillating system
β_y = dimensionless damping parameter for plunging system, $r_y/2m\omega_{ny}$
ρ = density of fluid
τ = dimensionless time for oscillating system, ω_{nyt}
τ^* = reduced dimensionless times for oscillating system, $\beta_y \tau$
ω_{ny} = natural circular frequency in plunging, $(k_y/m)^{1/2}$

Received December 6, 1971. The investigation reported here was supported by the National Research Council, Grant A-2181.

* Scientific Officer.

† Professor, Department of Mechanical Engineering. Member AIAA.

Introduction

THE vortex excited oscillations of aerodynamically bluff bodies, when exposed to a fluid stream, have been a subject of considerable study. To engineers, the prevention of aeroelastic vibrations of smoke stacks, transmission lines, suspension bridges, buildings, etc., is of particular interest. Angle section members used in open engineering structures, have been known to experience large amplitude oscillations when exposed to normal atmospheric winds, and in a few instances failure has been reported. The bluff geometry together with low natural frequency make these members susceptible to aeroelastic vibrations of vortex resonant or galloping nature. The character of the aerodynamic forces and the resulting instabilities have been discussed by the authors in the two recent papers.[1,2]

Often, as is the case with a structural angle beam, the instability at a given fluid stream velocity and angle of attack may be the combined effect of both vortex resonance and galloping. To permit the study of the individual forms of excitation, a judicious choice of either damping, angle section size or natural frequency is required to separate the two phenomena. At certain orientations of the angle section, it appeared that the vortex formation had some influence on the starting wind velocity, displacement amplitude and build-up time of the galloping instability. The present study explores the role of vortex formation during the galloping instability by isolating the former through the use of a splitter plate.

Experimental Set-Up and Discussion

Shown in Fig. 1 is a cross section of the angle model oriented at the angle of attack (α_0) of 45°, and the location of the splitter plate in the wake. Flow lines indicate typical instantaneous positions of the separated shear layers and the formation of shedded vortices if the splitter plate were absent. As reported by Arie and Rouse,[3] the formation of alternating vortices in the wake of a 3-in. flat plate located transverse to the freestream could be suppressed using a splitter plate 30 in. deep. Therefore, during the experimental tests with the 1-in. angle section, a 10-in. splitter plate was mounted at the downstream edge of the model causing the flow to reattach on the plate after initial separation at the corners of the model.

The experimental program was conducted in a low-speed, low-turbulence, return-type wind tunnel with a test section of $36 \times 27 \times 96$ in. A schematic of the model support system is shown in Fig. 2. The $1 \times 1 \times \frac{1}{4}$ in. angle section was mounted vertically on a system of journal bearings located on a frame encircling the tunnel test section. This gave the model a plunging degree of freedom lateral to the flow direction with structural and mean aerodynamic conditions essentially two-dimensional. Variable stiffness and damping were introduced through coil springs and electromagnetic eddy current dampers, respectively. The plunging displacement of the model was monitored using a variable inductance type of transducer.

A comparison of the representative gallping data, with and without the splitter plate, are summarized in Fig. 3 for the angle section at $\alpha_0 = 45°$. The results are expressed in terms of the non-dimensional displacement amplitude and build-up time vs the velocity parameter. Theoretical curves derived from a quasi-steady analysis[4] have been included to substantiate the validity of such an approach.

The results in absence of the splitter plate indicate that the influence of the vortex formation is to partially reduce the displacement amplitude and increase the time for build-up from rest at least over the initial velocity range conducive to galloping.

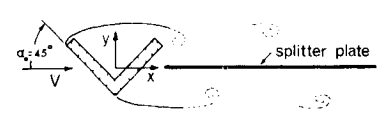

Fig 1 Angle section at 45° with separating shear layers and a splitter plate.